

Hybrid GFD-RBF Method for Convection-Diffusion Problems

Priyal Garg[†] and T.V.S. Sekhar^{*}

School of Basic Sciences, Indian Institute of Technology Bhubaneswar, Odisha-752050, India
[†]*a21ma09003@iitbbs.ac.in*, ^{*}*sekhartvs@iitbbs.ac.in*

Abstract

In this paper, we present a meshless hybrid method combining the Generalized Finite Difference (GFD) and Finite Difference based Radial Basis Function (RBF-FD) approaches to solve non-homogeneous partial differential equations (PDEs) involving both lower and higher order derivatives. The proposed method eliminates the need for mesh generation by leveraging the strengths of both GFD and RBF-FD techniques. The GFD method is robust and stable, effectively handling ill-conditioned systems, while the RBF-FD method excels in extending to higher-order derivatives and higher-dimensional problems. Despite their individual advantages, each method has its limitations. To address these, we developed a hybrid GFD-RBF approach that combines their strengths. Specifically, the GFD method is employed to approximate lower order terms (convective terms), and the RBF method is used for higher order terms (diffusive terms). The performance of the proposed hybrid method is tested on both linear and non-linear PDEs, considering uniform and non-uniform distributions of nodes within the domain. This approach demonstrates the versatility and effectiveness of the hybrid GFD-RBF method in solving second and higher order convection-diffusion problems.

Keywords : *Hybrid Meshless Method, Generalized Finite Difference Method, Radial Basis Function, GFD-RBF Method.*

1 Introduction

Non-homogeneous PDEs involving lower and higher order derivatives on complex or moving boundaries are frequently used to model various physical phenomena. Addressing the challenges posed by complex boundaries, meshless methods offer greater flexibility compared to mesh-based methods. By discretizing derivatives at scattered points without connecting them with edges, meshless methods are well-suited for problems involving moving boundaries, such as fluid-structure interaction. For boundary layer flows, adaptive local refinement is also straightforward, as there is no need to account for grid properties like control volume aspect ratio or element skewness. Recently, meshless numerical manifold method is also used for various physical problems [1, 2]. Localized meshless methods, such as GFD and RBF-FD have proven effective for these tasks.

GFD method is based on the Taylor series expansion and the moving least squares (MLS) technique for approximating the derivatives of an unknown function. Theoretical advancements in the GFD method were made by Jensen [3], Perrone and Kao [4], and Benito et al. [5], with subsequent analyses by Benito et al. [6] and Zheng and Li [7]. Applications of the GFD method have been demonstrated by Mochnacki and Majchrzak [8] and Urena et al. [9] across various

^{*}Corresponding Author

fields. Gavete et al. [10] applied the method to solve nonlinear elliptic PDEs, while Urena et al. [11, 12] tackled nonlinear parabolic and hyperbolic PDEs. GFD method has notable strengths, including its robustness and stability in handling ill-conditioned systems [13, 14]. However, it requires the computation of all derivatives of a particular order, even when only a few is needed for a specific PDE. Additionally, improving accuracy by including higher order terms in the Taylor series becomes computationally expensive due to the evaluation of numerous higher order derivatives. Consequently, GFD method is less efficient for solving higher order PDEs or achieving higher order accuracy. RBF-FD method [15–18], on the other hand, uses radial basis function interpolation to approximate derivatives at given points. It is well-suited for higher-order PDEs and high-dimensional problems, as demonstrated in various applications [19, 20] and modifications to the classical method [21–23]. The key advantage of the RBF-FD method lies in its extensibility and accuracy. However, its performance depends on selecting an optimal shape parameter. Further, if the number of nodes is increased beyond a certain limit, it can lead to discretization errors reaching a constant value, which is known as the stagnation or saturation phenomenon [22].

In general, numerical solutions for higher order PDEs are obtained by rewriting them as systems of lower order PDEs. However, this approach increases the number of unknowns and poses challenges in handling boundary conditions, particularly for complex boundaries. To address these issues, we have developed a hybrid GFD-RBF method that directly solves higher order PDEs by retaining the strengths of both GFD and RBF methods. In this hybrid approach, lower order derivatives (e.g., convection terms) are approximated using the GFD method, while higher order derivatives (e.g., diffusion terms) are computed using the RBF-FD method. The method has been tested on both linear and nonlinear PDEs, with a comparative analysis conducted with the standard second-order central finite difference (CD2) method for uniformly distributed nodes and GFD method for both uniform and non-uniform distributions.

2 Numerical Approximation

Consider a second-order non-homogenous partial differential equation of Dirichlet type:

$$\mathcal{L}(U(\mathbf{x})) = f(\mathbf{x}) \quad \text{in } \Omega \quad (1)$$

with boundary conditions

$$U(\mathbf{x}) = g(\mathbf{x}) \quad \text{on } \Gamma \quad (2)$$

where, $\mathbf{x} = (x, y)$.

Let n be the total number of nodes in the domain. The motive is to find the value of U at the internal nodes. For this, at each internal node, say \mathbf{x}_0 , define a composition with \mathbf{x}_0 as the central node and $\mathbf{x}_1, \mathbf{x}_2, \dots, \mathbf{x}_{N-1}$ as its neighbouring nodes. This composition is termed as star which is shown in Fig. 1. The star has been selected as per the quadrant rule [24].

In order to find the approximate value of $U(\mathbf{x})$, say $u(\mathbf{x})$, given PDE has to be discretized to get the corresponding difference equation. In hybrid GFD-RBF method, we propose that the lower order derivatives are approximated by GFD and the higher order derivatives by RBF-FD. For example, if a second order PDE is considered, the first order derivatives are approximated by GFD while the second order derivatives by RBF. Similarly, if a third order PDE is considered, first order derivatives are approximated by GFD and higher ones by RBF or derivatives up to second order are approximated by GFD and higher ones by RBF.

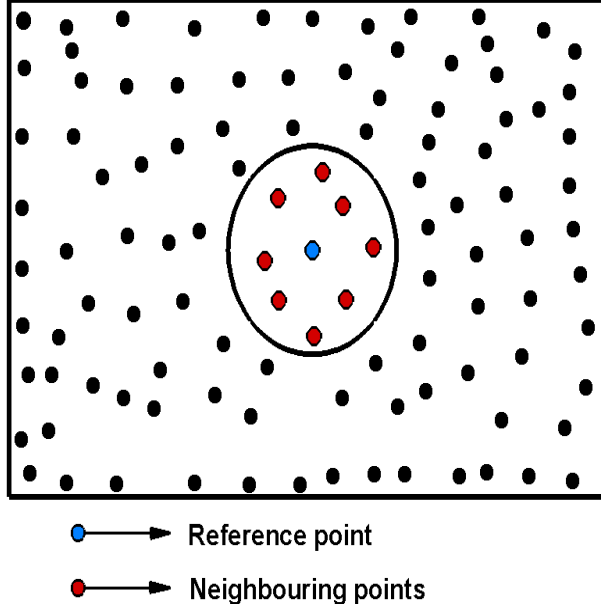


Figure 1: Domain showing star with central node and neighbouring nodes

2.1 Approximation of the First Order Derivatives by GFD

For a particular star, let $U(\mathbf{x}_0)$ is the value of the function at the central node and $U(\mathbf{x}_i)$, $i = 1, \dots, N-1$ are the function values at the neighbouring nodes, then according to the Taylor series expansion, we have:

$$U_i = U_0 + h_i \frac{\partial U_0}{\partial x} + k_i \frac{\partial U_0}{\partial y} + \dots, \quad i = 1, \dots, N-1, \quad (3)$$

$h_i = x_i - x_0$, $k_i = y_i - y_0$. If $u(\mathbf{x})$ be the approximate value of $U(\mathbf{x})$, then to get the approximations of first order, we truncate the series after first order terms. It can be represented in matrix form as:

$$\begin{bmatrix} h_1 & k_1 \\ h_2 & k_2 \\ \vdots & \vdots \\ h_{N-1} & k_{N-1} \end{bmatrix} \begin{bmatrix} \frac{\partial u_0}{\partial x} \\ \frac{\partial u_0}{\partial y} \end{bmatrix} = \begin{bmatrix} u_1 - u_0 \\ u_2 - u_0 \\ \vdots \\ u_{N-1} - u_0 \end{bmatrix},$$

or

$$AD_{\mathbf{u}_0} = \Delta \mathbf{u}. \quad (4)$$

Let

$$\mathbf{R} = \Delta \mathbf{u} - AD_{\mathbf{u}_0} \quad (5)$$

denotes the residue of Eq. (4). The residuals can be minimized by applying the MLS method. If $W = \text{diag}(w_1, w_2, \dots, w_{N-1})$ be the matrix of the weights, then according to the method we have to solve the following system of equations:

$$\frac{\partial \mathbf{R}' W^2 \mathbf{R}}{\partial D_{\mathbf{u}_0}} = 0. \quad (6)$$

The approximate values of the derivative can be obtained by solving Eq. (6) as:

$$D_{\mathbf{u}_0} = B\Delta\mathbf{u} \quad (7)$$

where,

$B = S^{-1}A'W^2$, $S = A'W^2A$. Using the quadrant criteria, the neighboring nodes around the central node are chosen in such a way that the matrix A contains a base of \mathbb{R}^2 , and hence S is invertible.

$$\text{Let } \mathbf{u} = (u_0, u_1, \dots, u_{N-1}) \text{ and } \bar{B} = \begin{bmatrix} -\sum_{i=1}^{N-1} b_{1,i} & b_{1,1} & b_{1,2} & \cdots & b_{1,N-1} \\ -\sum_{i=1}^{N-1} b_{2,i} & b_{2,1} & b_{2,2} & \cdots & b_{2,N-1} \end{bmatrix}$$

where, $b_{i,j}$ are the elements of B . Now the expression for the derivatives will be given by

$$D_{\mathbf{u}_0} = B\Delta\mathbf{u} = \bar{B}\mathbf{u} = \begin{bmatrix} -u_0 \sum_{i=1}^{N-1} b_{1,i} + \sum_{i=1}^{N-1} b_{1,i}u_i \\ -u_0 \sum_{i=1}^{N-1} b_{2,i} + \sum_{i=1}^{N-1} b_{2,i}u_i \end{bmatrix}. \quad (8)$$

The above equation will give the discretized form of the first order derivatives at an internal node (\mathbf{x}_0) of a star of the domain. The same process is repeated by considering each internal node as the central node and assigning a star to that node.

2.2 Approximation of the Second Order Derivatives by RBF-FD

Let's consider the same star as for GFD with N distinct nodes. If $u(\mathbf{x})$ be the approximate value of $U(\mathbf{x})$, then the RBF interpolation is given by

$$u(\mathbf{x}) \approx s(\mathbf{x}) = \sum_{i=0}^{N-1} \lambda_i \phi(\|\mathbf{x} - \mathbf{x}_i\|, \epsilon) + \sum_{j=0}^{M-1} \mu_j p_j(\mathbf{x}) \quad (9)$$

where, ϕ is the RBF function with ϵ as the shape parameter and $\{p_j(\mathbf{x})\}_{j=0}^{M-1}$ is a basis for $\Pi_M(\mathbb{R}^2)$ (space of all 2-variate polynomials of degree less than or equals to M) which is required for the interpolation problem to be well-posed [25]. Putting $u(\mathbf{x}_i) = s(\mathbf{x}_i)$, $i = 0, \dots, N-1$ in Eq. (9), we get N linear equations and therefore M extra conditions are required to solve the equation. These extra conditions are chosen by taking the expansion coefficient vector $\lambda \in \mathbb{R}^N$ orthogonal to $\Pi_M(\mathbb{R}^2)$, i.e.,

$$\sum_{i=0}^{N-1} \lambda_i p_j(\mathbf{x}_i) = 0, \quad j = 0, \dots, M-1.$$

This will lead to a system of linear equations which can be represented as:

$$\begin{bmatrix} \phi & \mathbf{p} \\ \mathbf{p} & \mathbf{0} \end{bmatrix} \begin{bmatrix} \lambda \\ \mu \end{bmatrix} = \begin{bmatrix} \mathbf{u} \\ \mathbf{0} \end{bmatrix} \quad (10)$$

where, $\phi := \phi(\|\mathbf{x}_j - \mathbf{x}_i\|, \epsilon)$, $i, j = 0, \dots, N-1$ and $\mathbf{p} := p_j(\mathbf{x}_i)$, $j = 0, \dots, M-1$, $i = 0, \dots, N-1$.

In order to derive the derivatives of the function $u(\mathbf{x})$ at a given point, Lagrange form of

RBF interpolant is used which is given by

$$u(\mathbf{x}) \approx s(\mathbf{x}) = \sum_{i=0}^{N-1} \psi_i(\mathbf{x})u(\mathbf{x}_i) \quad (11)$$

where, $\psi_i(\mathbf{x})$ satisfies the condition of Kronecker delta, i.e.,

$$\psi_i(\mathbf{x}_j) = \delta_{ij}, \quad j = 0, \dots, N-1. \quad (12)$$

The closed form representation for $\psi_i(\mathbf{x})$ can be obtained by considering that the right-hand side vector of Eq. (10) stems from each ψ_i 's. Hence,

$$\psi_i(\mathbf{x}) = \frac{\det(Q_i(\mathbf{x}))}{\det(Q)} \quad (13)$$

where,

$$Q = \begin{bmatrix} \phi & \mathbf{p} \\ \mathbf{p} & \mathbf{0} \end{bmatrix} \quad (14)$$

and $Q_i(\mathbf{x})$ is same as the matrix Q , except that the i th row is replaced by the vector

$$B(\mathbf{x}) = [\phi(\|\mathbf{x} - \mathbf{x}_0\|, \epsilon), \dots, \phi(\|\mathbf{x} - \mathbf{x}_{N-1}\|, \epsilon) \mid p_0(\mathbf{x}), \dots, p_{M-1}(\mathbf{x})]. \quad (15)$$

The representations through Eqs. (11-14) can be used to approximate the derivative of a function $\mathbf{L}u$ at a given point \mathbf{x}_j , where \mathbf{L} is a second order linear differential operator. To derive the formulae for $\mathbf{L}(u(\mathbf{x}_0))$, a set of neighboring node of \mathbf{x}_0 (say $\{\mathbf{x}_0, \mathbf{x}_1, \dots, \mathbf{x}_{N-1}\}$) is considered. Let $\mathbf{L}(u(\mathbf{x}_0))$ be represented as a linear combination of the value of u at \mathbf{x}_0 and its neighbouring nodes, i.e.,

$$\mathbf{L}(u(\mathbf{x}_0)) = \sum_{i=0}^{N-1} c_i u(\mathbf{x}_i), \text{ for each } \mathbf{x}_0 \in \Omega \quad (16)$$

where, c_i 's are the weights to be calculated. So, after applying the operator \mathbf{L} to the Lagrange form of RBF interpolant in Eq. (11) for \mathbf{x}_0 , we get

$$\mathbf{L}(u(\mathbf{x}_0)) \approx \mathbf{L}(s(\mathbf{x}_0)) = \sum_{i=0}^{N-1} \mathbf{L}(\psi_i(\mathbf{x}_0))u(\mathbf{x}_i). \quad (17)$$

On comparing Eqs. (16-17), we get c_i 's as:

$$c_i = \mathbf{L}(\psi_i(\mathbf{x}_0)), \quad i = 0, \dots, N-1. \quad (18)$$

The weights can be computed by solving the following linear system:

$$Q[\mathbf{c}/\boldsymbol{\mu}] = (\mathbf{L}(B(\mathbf{x}_0)))^T, \text{ for each } \mathbf{x}_0 \in \Omega \quad (19)$$

where, Q and B are given by Eq. (14) and Eq. (15) respectively and $c = [c_0, c_2, \dots, c_{N-1}]^T$ denotes the vector of weights.

Putting the values of weights in Eq. (16) will give the discretized form of the second order derivatives at an internal node of the domain. The same process is repeated for each internal node of the domain.

Substituting the value of first order derivatives obtained from GFD and the second order derivatives obtained from RBF-FD for a given node in Eq. (1), we get an algebraic equation corresponding to that node. The same process is repeated for each internal node of the domain to get a system of equations in which the number of equations and unknowns will be equal to the number of internal nodes. This algebraic system is solved using the stabilized bi-conjugate gradient (Bi-CGSTAB) method to obtain the approximate value of the function U at each node of the domain.

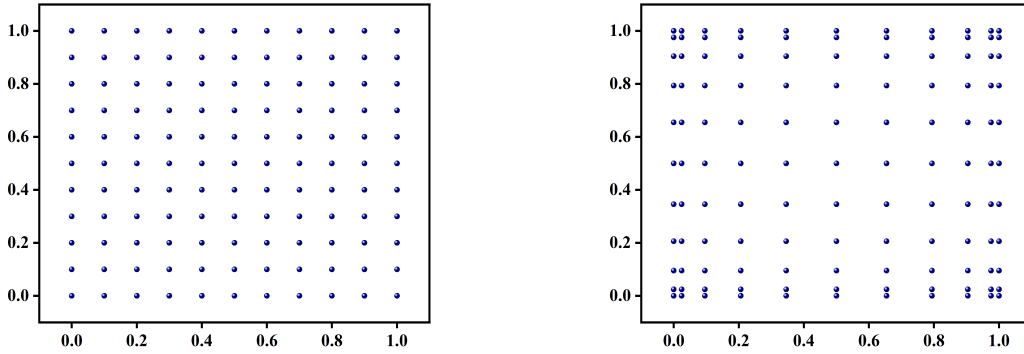
3 Results and Discussion

The hybrid method has been applied to both linear and nonlinear PDEs with known analytical solutions. Boundary conditions and the source terms can be calculated from the analytical solution wherever required. Domains are discretized by considering uniform and Chebyshev distribution of nodes. The sample of 2D domains with chosen points is shown in Fig. 2. Chebyshev nodes are generated by using the formula:

$$x_i = \frac{1}{2} \left[1 - \cos \left(\frac{i-1}{n_x-1} \cdot \pi \right) \right], \quad i = 1, \dots, n_x,$$

$$y_j = \frac{1}{2} \left[1 - \cos \left(\frac{j-1}{n_y-1} \cdot \pi \right) \right], \quad j = 1, \dots, n_y.$$

The weight function for GFD is taken as $1/(\text{distance})^2$ and multiquadric function $(\sqrt{1 + \epsilon^2 r^2})$ [26] is used for RBF-FD.



(a) Uniform Nodes

(b) Chebyshev Nodes

Figure 2: Discretization of the Domain with 121 Nodes

3.1 Illustrative Examples

Example 1: Linear Convection-Diffusion Equation

$$-2 \frac{\partial U}{\partial x} + 2 \frac{\partial U}{\partial y} - \frac{\partial^2 U}{\partial x^2} - \frac{\partial^2 U}{\partial y^2} = f(x, y), \quad 0 \leq x, y \leq 1.$$

Exact solution:

$$U(x, y) = \frac{e^{2(1-x)} + e^{2y} - 2}{e - 1}.$$

Table 1: Comparison of Error, Order of Convergence and Condition Number of the Stiffness Matrix for Example 1 with $\epsilon = 0.5$

Nodes	Hybrid GFD-RBF			CD2			Ref. [27]*(RBF-FD)	
	Error	Order	C.N.	Error	Order	C.N.	Error	Order
121	3.4543×10^{-5}	-	38.3205	2.1827×10^{-4}	-	38.3125	1.3257×10^{-3}	-
441	8.9838×10^{-6}	1.9429	154.8495	5.8404×10^{-5}	1.9019	154.8409	3.7435×10^{-4}	1.82
1681	2.2998×10^{-6}	1.9658	620.9606	1.9312×10^{-5}	1.5965	620.9518	9.1949×10^{-5}	2.02

*Number of nodes taken by the authors for RBF-FD are 81, 289 and 1089.

In Example 1, the proposed hybrid method has been applied to linear convection-diffusion equation by discretizing the convective terms using GFD and the diffusive terms by RBF with five nodes per star ($N_G = 5$, $N_R = 5$) as described in Section 2. To analyse the efficiency of the hybrid method, the root mean square (RMS) error (using analytical solution), order of convergence of the method and the condition number (C.N.) of the stiffness matrix with uniform distribution of nodes are calculated and presented in Table 1. The order of convergence of the method is given by

$$q \approx \frac{\log(e_{\text{old}} - e_{\text{new}})}{\log(h_{\text{old}} - h_{\text{new}})}$$

where, e_{old} and e_{new} are the RMS errors with nodal spacing h_{old} and h_{new} respectively. The condition number of stiffness matrix is calculated since the stability of a system of algebraic equations is closely related to the condition number of its coefficient matrix. The proposed hybrid method is compared with CD2 and RBF-FD [27] methods and the results are given in Table 1. It is found that the hybrid method gives more accurate results and it is second order accurate. In fact, the developed hybrid method is giving more satisfactory results with less number of nodes (e.g. nodes-121, error- 3.4543×10^{-5}) in the domain when compared with RBF-FD (e.g. nodes-289, error- 3.7435×10^{-4}). The condition number of the stiffness matrix of the hybrid method and CD2 is also comparable with each other.

Table 2: Comparison of Error and Order of Convergence for Different Nodes per Star for Uniform Distribution of Nodes for Example 1 with $\epsilon = 0.5$

Nodes	$N_G = 5, N_R = 5$		$N_G = 9, N_R = 5$		$N_G = 9, N_R = 9$	
	Error	Order	Error	Order	Error	Order
121	3.4543×10^{-5}	-	3.4601×10^{-5}	-	1.4893×10^{-4}	-
441	8.9838×10^{-6}	1.9429	8.9878×10^{-6}	1.9447	4.1394×10^{-5}	1.8471
1681	2.2998×10^{-6}	1.9658	1.2300×10^{-6}	1.9662	2.4561×10^{-5}	0.7530

In order to study the influence of the number of nodes per star around the central node in the hybrid method, three different types of stars, namely, five nodes per star for both GFD and RBF ($N_G = 5$, $N_R = 5$), nine nodes per star for GFD and five nodes for RBF ($N_G = 9$, $N_R = 5$) and nine nodes per star for both GFD and RBF ($N_G = 9$, $N_R = 9$) are considered. The RMS error and order of convergence of these three stars have been calculated for both uniform and Chebyshev distribution of nodes and are tabulated in Tables 2 and 3 respectively. For

Table 3: Comparison of Error and Order of Convergence for Different Nodes per Star for Chebyshev Distribution of Nodes for Example 1 with $\epsilon = 0.9$

Nodes	$N_G = 5, N_R = 5$		$N_G = 9, N_R = 5$		$N_G = 9, N_R = 9$	
	Error	Order	Error	Order	Error	Order
121	6.4167×10^{-4}	-	4.0826×10^{-4}	-	5.0923×10^{-4}	-
441	1.6445×10^{-4}	1.9823	1.0243×10^{-4}	2.0134	1.3785×10^{-4}	1.9190
1681	4.1914×10^{-5}	1.9783	2.5968×10^{-5}	1.9876	N.C.*	-

*Not Convergent

Table 4: Comparison of CPU Time for Different Nodes per Star for Uniform Distribution of Nodes for Example 1

Nodes	$N_G = 5, N_R = 5$	$N_G = 9, N_R = 5$	$N_G = 9, N_R = 9$
121	2.5625×10^{-2}	6.2500×10^{-2}	7.8126×10^{-2}
441	0.2343	0.4062	0.6093
1861	3.4687	4.1718	5.2812

Table 5: Comparison of CPU Time for Different Nodes per Star for Chebyshev Distribution of Nodes for Example 1

Nodes	$N_G = 5, N_R = 5$	$N_G = 9, N_R = 5$	$N_G = 9, N_R = 9$
121	6.2500×10^{-2}	9.3750×10^{-2}	0.1562
441	2.6250	4.2968	594.9375
1861	115.2968	144.75	-

Chebyshev distribution of nodes, nodal spacing is calculated by using the formula:

$$h = \max_{1 \leq i \leq n} \min_{1 \leq j \leq n, j \neq i} |\mathbf{x}_i - \mathbf{x}_j|.$$

In case of uniform distribution, the error and order of convergence with $(N_G = 5, N_R = 5)$ and $(N_G = 9, N_R = 5)$ are comparable, showing no significant difference. On the other hand, $(N_G = 9, N_R = 9)$ lags behind the other two types of stars both in error and order of convergence. Similar results are noticed with Chebyshev distribution of nodes as can be seen in Table 3. The CPU time taken for convergence for all three types of stars are tabulated in Tables 4 and 5. It is clear from both the tables that the CPU time taken by $(N_G = 5, N_R = 5)$ is much less than the other two stars, proving that $(N_G = 5, N_R = 5)$ produces the most efficient results.

The efficiency of the hybrid GFD-RBF $(N_G = 5, N_R = 5)$ is also compared with GFD $(N_G = 9)$ for both types of nodal distributions in the domain and tabulated in Tables 6-9. It has been found from Tables 6 and 7 that hybrid method is producing more accurate results than GFD method. Tables 8 and 9 show that hybrid method is able to save a significant amount of CPU time compared with GFD method. The maximum CPU time saving with hybrid method is 20.26% in the case of uniform distribution of nodes and 33.33% in the case of Chebyshev nodes. Hence hybrid GFD-RBF $(N_G = 5, N_R = 5)$ method proves to be an efficient meshless method to solve the linear convection-diffusion problems.

Table 6: Comparison of Error and Order of Convergence for Hybrid GFD-RBF and GFD for Uniform Distribution of Nodes for Example 1

Nodes	Hybrid GFD-RBF		GFD	
	Error	Order	Error	Order
121	3.4543×10^{-5}	-	2.2081×10^{-4}	-
441	8.9838×10^{-6}	1.9429	5.7462×10^{-5}	1.9421
1681	2.2998×10^{-6}	1.9658	1.4693×10^{-5}	1.9674

Table 7: Comparison of Error and Order of Convergence for Hybrid GFD-RBF and GFD for Chebyshev Distribution of Nodes for Example 1

Nodes	Hybrid GFD-RBF		GFD	
	Error	Order	Error	Order
121	6.4167×10^{-4}	-	6.5959×10^{-4}	-
441	1.6445×10^{-4}	1.9823	1.6942×10^{-4}	1.9792
1681	4.19146×10^{-5}	1.9783	4.3183×10^{-5}	1.9793

Table 8: Comparison of CPU Time for Hybrid GFD-RBF and GFD for Uniform Distribution of Nodes for Example 1

Nodes	Hybrid GFD-RBF	GFD	Time saved with Hybrid (w.r.t. GFD)
121	2.5625×10^{-2}	3.1250×10^{-2}	18%
441	0.2343	0.2900	19.20%
1861	2.7656	3.4687	20.26%

Table 9: Comparison of CPU Time for Hybrid GFD-RBF and GFD for Chebyshev Distribution of Nodes for Example 1

Nodes	Hybrid GFD-RBF	GFD	Time saved with Hybrid (w.r.t. GFD)
121	6.2500×10^{-2}	9.3750×10^{-2}	33.33%
441	2.6250	3.8593	31.9824%
1861	115.2968	158.3750	27.2001%

Example 2: Nonlinear Convection-Diffusion Equation

$$\left(\frac{\partial U}{\partial x}\right)^2 + \left(\frac{\partial U}{\partial y}\right)^2 + U \left(\frac{\partial^2 U}{\partial x^2} + \frac{\partial^2 U}{\partial y^2}\right) = 2U^4, \quad 0 \leq x, y \leq 1.$$

Exact solution:

$$U(x, y) = \frac{1}{\sqrt{(x+1)^2 + (y+1)^2}}.$$

In Example 2, the hybrid GFD-RBF method has been applied to nonlinear convection-

Table 10: Comparison of Error, Order of Convergence and Condition Number of the Stiffness Matrix for Example 2 with $\epsilon = 0.6$

Nodes	Hybrid GFD-RBF			CD2		
	Error	Order	C.N.	Error	Order	C.N.
121	9.9818×10^{-6}	-	45.1127	5.1342×10^{-5}	-	45.1101
441	2.6321×10^{-6}	1.9320	199.1313	1.3633×10^{-5}	1.9129	199.1288
1681	7.3073×10^{-7}	1.8488	852.0021	3.59178×10^{-6}	1.9244	851.9988

diffusion equation. In this example, the numerical solution obtained by the hybrid method ($N_G = 5$, $N_R = 5$) is closer to the analytical solution than CD2 as observed in Table 10. The order of convergence and condition number of the stiffness matrix are in agreement with each other for both the methods. The error produced by hybrid method is also in line with GFD method as mentioned in Reference [10].

Table 11: Comparison of Error and Order of Convergence for Different Nodes per Star for Uniform Distribution of Nodes for Example 2 with $\epsilon = 0.6$

Nodes	$N_G = 5$, $N_R = 5$		$N_G = 9$, $N_R = 5$		$N_G = 9$, $N_R = 9$	
	Error	Order	Error	Order	Error	Order
121	9.9818×10^{-6}	-	4.5601×10^{-5}	-	1.1396×10^{-4}	-
441	2.6321×10^{-6}	1.9230	1.1290×10^{-5}	2.0142	3.5334×10^{-5}	1.6894
1681	7.3073×10^{-7}	1.8488	1.9550×10^{-6}	2.5298	8.2526×10^{-6}	2.0981

Table 12: Comparison of Error and Order of Convergence for Different Nodes per Star for Chebyshev Distribution of Nodes for Example 2 with $\epsilon = 0.5$

Nodes	$N_G = 5$, $N_R = 5$		$N_G = 9$, $N_R = 5$		$N_G = 9$, $N_R = 9$	
	Error	Order	Error	Order	Error	Order
121	2.7062×10^{-5}	-	5.6769×10^{-5}	-	5.8346×10^{-5}	-
441	6.5296×10^{-6}	2.0702	1.4599×10^{-5}	1.9775	N.C.	-
1681	1.4256×10^{-6}	2.2035	3.8659×10^{-6}	1.9240	N.C.	-

Table 13: Comparison of CPU Time for Different Nodes per Star for Uniform Distribution of Nodes for Example 2

Nodes	$N_G = 5$, $N_R = 5$	$N_G = 9$, $N_R = 5$	$N_G = 9$, $N_R = 9$
121	0.3281	0.6875	1.0937
441	2.9687	6.8125	11.2812
1861	30.4375	89.6562	160.5156

When the number of nodes in a star is increased, it is observed from Table 11 that in case of uniform distribution, ($N_G = 5$, $N_R = 5$) has less error than ($N_G = 9$, $N_R = 5$) though

Table 14: Comparison of CPU Time for Different Nodes per Star for Chebyshev Distribution of Nodes for Example 2

Nodes	$N_G = 5, N_R = 5$	$N_G = 9, N_R = 5$	$N_G = 9, N_R = 9$
121	0.4531	1.7343	1.9062
441	14.0345	73.2812	-
1861	684.2656	4752.2656	-

the order of convergence is high in $(N_G = 9, N_R = 5)$. On the other hand, RMS error and order of convergence produced by $(N_G = 9, N_R = 9)$ are not as satisfactory as with the other two types of stars. In case of Chebyshev distribution of nodes, $(N_G = 5, N_R = 5)$ is giving more accurate results, as is seen from Table 12. It is also clear from Tables 13 and 14 that $(N_G = 5, N_R = 5)$ is computationally efficient as the CPU time taken is less than the other two.

Table 15: Comparison of Error and Order of Convergence for Hybrid GFD-RBF and GFD for Uniform Distribution of Nodes for Example 2

Nodes	Hybrid GFD-RBF		GFD	
	Error	Order	Error	Order
121	9.9818×10^{-6}	-	7.9030×10^{-5}	-
441	2.6321×10^{-6}	1.9230	2.0600×10^{-5}	1.9397
1681	7.3073×10^{-7}	1.8488	5.1814×10^{-6}	1.9952

Table 16: Comparison of Error and Order of Convergence for Hybrid GFD-RBF and GFD for Chebyshev Distribution of Nodes for Example 2

Nodes	Hybrid GFD-RBF		GFD	
	Error	Order	Error	Order
121	2.7062×10^{-5}	-	9.8615×10^{-5}	-
441	6.5296×10^{-6}	2.0702	2.5439×10^{-5}	1.9730
1681	1.4256×10^{-6}	2.2035	5.8435×10^{-6}	2.1299

Table 17: Comparison of CPU Time for Hybrid GFD-RBF and GFD for Uniform Distribution of Nodes for Example 2

Nodes	Hybrid GFD-RBF	GFD	Time saved with Hybrid (w.r.t. GFD)
121	0.3281	0.4218	22.21%
441	2.9687	3.8625	23.14%
1861	30.4375	40.0312	23.96%

The RMS error and the order of convergence of hybrid method $(N_G = 5, N_R = 5)$ are compared with GFD for both types of nodal distributions and results are tabulated in Tables

Table 18: Comparison of CPU Time for Hybrid GFD-RBF and GFD for Chebyshev Distribution of Nodes for Example 2

Nodes	Hybrid GFD-RBF	GFD	Time saved with Hybrid (w.r.t. GFD)
121	0.4531	0.8437	46.29%
441	14.0345	26.7343	47.50%
1861	684.2656	1329.9220	48.54%

15 and 16. It is found from the tables that the hybrid method gives more accurate results than GFD method while maintaining the same level of order of convergence. Comparison of CPU time for both the methods is also done which is given in Tables 17 and 18. It is found that hybrid method is able to save a maximum CPU time of 23.96% in the case of uniform nodes and 48.54% in the case of Chebyshev nodes. Hence, the developed hybrid GFD-RBF ($N_G = 5, N_R = 5$) method solves nonlinear convection-diffusion problem efficiently.

Example 3: Coupled Nonlinear Convection-Diffusion Equation

$$\begin{aligned}
 U \frac{\partial U}{\partial x} + V \frac{\partial U}{\partial y} - \frac{\partial^2 U}{\partial x^2} - \frac{\partial^2 U}{\partial y^2} &= f_1(x, y), \\
 U \frac{\partial V}{\partial x} + V \frac{\partial V}{\partial y} - \frac{\partial^2 V}{\partial x^2} - \frac{\partial^2 V}{\partial y^2} &= f_2(x, y),
 \end{aligned}
 \quad 0 \leq x, y \leq \pi.$$

Exact solution:

$$U(x, y) = -\cos x \sin y, \quad V(x, y) = \sin x \cos y.$$

Table 19: Comparison of Error, Order of Convergence and Condition Number of the Stiffness Matrix for Example 3 with $\epsilon = 0.3$

Nodes	Hybrid GFD-RBF			CD2			Ref. [27](RBF-FD)		
	Error	Order	C.N.	Error	Order	C.N.	Error	Order	
u	121	3.6074×10^{-4}	-	38.8377	9.7989×10^{-4}	-	38.8193	4.8366×10^{-4}	-
	441	9.2307×10^{-5}	1.9664	156.8412	2.5603×10^{-4}	1.9363	156.8192	1.1976×10^{-4}	2.01
	1681	2.3507×10^{-5}	1.9733	628.8272	6.5524×10^{-5}	1.9662	628.8043	3.0248×10^{-5}	2.71
v	121	6.5152×10^{-4}	-	38.8377	2.5574×10^{-4}	-	38.8193	1.0350×10^{-3}	-
	441	1.7188×10^{-4}	1.9224	156.8412	6.8869×10^{-5}	1.8927	156.8192	2.7923×10^{-4}	1.89
	1681	4.4140×10^{-5}	1.9612	628.8272	1.7715×10^{-5}	1.9588	628.8043	2.4539×10^{-4}	0.19

The developed hybrid method is also tested on coupled nonlinear convection-diffusion equation in Example 3. The comparison of the hybrid method is done with CD2 and RBF-FD [27] methods in terms of error, order of convergence and condition number of the stiffness matrix and the results are tabulated in Table 19. It is found the numerical solution obtained by the proposed hybrid method is more accurate than the other two methods. The order of convergence and condition number of the hybrid method is in agreement with the other two methods.

The influence of the number of nodes per star in the hybrid method has been studied for uniform and Chebyshev distribution of nodes in the domain. Table 20 shows that, ($N_G =$

Table 20: Comparison of Error and Order of Convergence for Different Nodes per Star for Uniform Distribution of Nodes for Example 3 with $\epsilon = 0.3$

Nodes	$N_G = 5, N_R = 5$		$N_G = 9, N_R = 5$		$N_G = 9, N_R = 9$		
	Error	Order	Error	Order	Error	Order	
u	121	3.6074×10^{-4}	-	1.3650×10^{-3}	-	1.1579×10^{-2}	-
	441	9.2307×10^{-5}	1.9664	3.5707×10^{-4}	1.9346	5.4368×10^{-3}	1.0906
	1681	2.3507×10^{-5}	1.9733	9.1420×10^{-5}	1.9656	2.6093×10^{-3}	1.0590
v	121	6.5152×10^{-4}	-	3.7985×10^{-4}	-	9.8660×10^{-3}	-
	441	1.7188×10^{-4}	1.9224	9.7175×10^{-5}	1.9667	3.2541×10^{-3}	1.6002
	1681	4.4140×10^{-5}	1.9612	2.4759×10^{-5}	1.9726	1.0056×10^{-3}	1.6942

Table 21: Comparison of Error and Order of Convergence for Different Nodes per Star for Chebyshev Distribution of Nodes for Example 3 with $\epsilon = 0.3$

Nodes	$N_G = 5, N_R = 5$		$N_G = 9, N_R = 5$		$N_G = 9, N_R = 9$		
	Error	Order	Error	Order	Error	Order	
u	121	8.4971×10^{-4}	-	1.8755×10^{-3}	-	1.5195×10^{-2}	-
	441	2.1565×10^{-4}	1.9967	4.8936×10^{-4}	1.9564	N.C.	-
	1681	5.4810×10^{-5}	1.9834	1.2522×10^{-4}	1.9737	N.C.	-
v	121	9.8395×10^{-4}	-	4.8010×10^{-4}	-	2.6727×10^{-2}	-
	441	2.8839×10^{-4}	1.7871	1.2765×10^{-4}	1.8954	N.C.	-
	1681	7.6075×10^{-5}	1.9283	3.2857×10^{-5}	1.9651	N.C.	-

Table 22: Comparison of CPU Time for Different Nodes per Star for Uniform Distribution of Nodes for Example 3

Nodes	$N_G = 5, N_R = 5$	$N_G = 9, N_R = 5$	$N_G = 9, N_R = 9$
121	3.1250×10^{-2}	0.1562	0.4062
441	0.5781	2.2500	7.0156
1861	7.8281	35.2500	104.2500

Table 23: Comparison of CPU Time for Different Nodes per Star for Chebyshev Distribution of Nodes for Example 3

Nodes	$N_G = 5, N_R = 5$	$N_G = 9, N_R = 5$	$N_G = 9, N_R = 9$
121	0.1718	0.4843	0.8593
441	5.8593	22.0156	-
1861	271.2187	1396.4687	-

5, $N_R = 5$) has less error than ($N_G = 9, N_R = 5$) in case of uniform distribution of nodes while maintaining the same level of order of convergence. On the other hand, ($N_G = 9, N_R = 9$) has low performance than the other two methods. Similar results are there for Chebyshev distribution of nodes, as is seen from Table 21. The CPU time taken by ($N_G = 5, N_R = 5$) is also less

than the other two stars in both types of nodal distributions, as observed from Tables 22 and 23, proving its efficiency over the other two methods.

Table 24: Comparison of Error and Order of Convergence for Hybrid GFD-RBF and GFD for Uniform Distribution of Nodes for Example 3

Nodes	Hybrid GFD-RBF		GFD		
	Error	Order	Error	order	
u	121	3.6074×10^{-4}	-	2.2484×10^{-3}	-
	441	9.2307×10^{-5}	1.9664	5.8221×10^{-4}	1.9492
	1681	2.3507×10^{-5}	1.9733	1.4865×10^{-4}	1.9676
v	121	6.5152×10^{-4}	-	8.7300×10^{-4}	-
	441	1.7188×10^{-4}	1.9224	2.3464×10^{-4}	1.8955
	1681	4.4140×10^{-5}	1.9612	6.0088×10^{-5}	1.9653

Table 25: Comparison of Error and Order of Convergence for Hybrid GFD-RBF and GFD for Chebyshev Distribution of Nodes for Example 3

Nodes	Hybrid GFD-RBF		GFD		
	Error	Order	Error	order	
u	121	8.4971×10^{-4}	-	3.1552×10^{-3}	-
	441	2.1565×10^{-4}	1.9967	8.0597×10^{-4}	1.9873
	1681	5.4810×10^{-5}	1.9834	2.0513×10^{-4}	1.9769
v	121	8.4971×10^{-4}	-	1.6287×10^{-3}	-
	441	2.8839×10^{-4}	1.7871	4.1602×10^{-4}	1.9873
	1681	7.6075×10^{-5}	1.9283	1.0584×10^{-4}	1.9822

Table 26: Comparison of CPU Time for Hybrid GFD-RBF and GFD for Uniform Distribution of Nodes for Example 3

Nodes	Hybrid GFD-RBF	GFD	Time saved with Hybrid (w.r.t. GFD)
121	3.1250×10^{-2}	3.6825×10^{-2}	15.13%
441	0.5781	0.5312	-8.82%
1861	7.8281	7.1187	-9.96%

Numerical solution obtained by hybrid method ($N_G = 5$, $N_R = 5$) is more accurate than GFD as is evident from Tables 24 and 25. With the increase of number of nodes in the uniform distribution, it is observed that the hybrid method needs more CPU time than GFD as shown in Table 26. But it is able to save a maximum of 47.44% CPU time in case of Chebyshev distribution of nodes as mentioned in Table 27. So in general, for solving coupled nonlinear convection-diffusion problems, hybrid GFD-RBF ($N_G = 5$, $N_R = 5$) proved to be an efficient meshless method.

Table 27: Comparison of CPU Time for Hybrid GFD-RBF and GFD for Chebyshev Distribution of Nodes for Example 3

Nodes	Hybrid GFD-RBF	GFD	Time saved with Hybrid (w.r.t. GFD)
121	0.1718	0.2187	21.44%
441	5.8593	9.7187	39.71%
1861	271.2187	516.0625	47.44%

4 Conclusion

Hybrid GFD-RBF method has been tested on linear and nonlinear convection-diffusion problems for both uniform and non-uniform distributions of nodes. For uniform node distribution, it was compared with the second-order central finite difference (CD2) method. Results show that the hybrid method produces significantly smaller errors than CD2 across all tested problems. Furthermore, the condition number of the stiffness matrix obtained from the hybrid method was evaluated and found to be satisfactory in comparison to CD2. It was observed that the hybrid method achieves optimal results with five nodes per star ($N_G = 5$, $N_R = 5$) for both uniform and non-uniform node distributions, whereas the GFD method requires nine nodes. Despite using fewer nodes per star, the hybrid method gives more accurate results than the GFD method. Additionally, in cases involving non-uniform node distributions, the hybrid method requires less CPU time than the GFD method. The hybrid method was determined to be numerically second order accurate. But the limitation of the method is that it is not helpful if the PDE is of homogenous type.

So, the hybrid method would be more effective if the first order derivatives (convective terms) are discretized by GFD and higher order derivatives (diffusive and other higher order terms) by RBF-FD to solve non-homogenous PDEs. Hence the developed method is computationally efficient and hence useful in solving convection-diffusion equations especially where the convective terms are highly nonlinear.

References

- [1] Hongwei, G., Shan, L., Hong, Z. [2023] "GMLS-based numerical manifold method in mechanical analysis of thin plates with complicated shape or cutouts," *Eng. Anal. Bound. Elem.* **151**, 597-623.
- [2] Xitailang, C., Shan, L., Zenglong, L., Hongwei, G., Hong, Z. [2024] "Meshless numerical manifold method with novel subspace tracking and CSS locating techniques for slope stability analysis," *Comput. Geotech.* **166**, 106025.
- [3] Jensen, P.S. [1972] "Finite difference technique for variable grid," *Comput. & Structures* **2**, 17-29.
- [4] Perrone, N., Kao, R. [1975] "A general finite difference method for arbitrary meshes," *Comput. & Structures* **5**, 45-58.

- [5] Benito, J.J., Ureña, F., Gavete, L. [2001] “Influence several factors in the generalized finite difference method,” *Appl. Math. Modelling* **25**, 1039–1053.
- [6] Benito, J.J., Ureña, F., Gavete, L., Alonso, B. [2009] “Application of the generalized finite difference method to improve the approximated solution of pdes,” *Comput. Model. Eng. Sci.* **38**, 39–58.
- [7] Zheng, Z., Li, X. [2022] “Theoretical analysis of the generalized finite difference method,” *Comput. Math. Appl.* **120**, 1-14.
- [8] Mochnacki, B., Majchrzak, E. [2010] “Numerical modeling of casting solidification using generalized finite difference method,” *Mater. Sci. Forum* **638–642**, 2676–2681.
- [9] Ureña, F., Benito, J.J., Gavete, L. [2011] “Application of the generalized finite difference method to solve the advection-diffusion equation,” *J. Comput. Appl. Math.* **235**, 1849–1855.
- [10] Gavete, L., Ureña, F., Benito, J.J., García, A., Ureña, M., Saletе, E. [2017] “Solving second order non-linear elliptic partial differential equations using generalized finite difference method,” *J. Comput. Appl. Math.* **318**, 378–387.
- [11] Ureña, F., Gavete, L., García, A., Benito, J.J., Vargas, A.M. [2019] “Solving second order non-linear parabolic PDEs using generalized finite difference method (GFDM),” *J. Comput. Appl. Math.* **354**, 221-241.
- [12] Ureña, F., Gavete, L., García, A., Benito, J.J., Vargas, A.M. [2020] “Solving second order non-linear hyperbolic PDEs using generalized finite difference method (GFDM),” *J. Comput. Appl. Math.* **363**, 1-21.
- [13] Haung, T., Zhao, H., Chen, H., Yao, Y., Yu, P. [2022] “A hybrid cartesian-meshless method for the simulatrion of thermal flows with complex immersed objects,” *Phys. Fluids* **34**, 103318.
- [14] Wright, G.B., Jones, A., Shankar, V. [2023] “MGM: A meshfree geometric multilevel method for systems arising from elliptic equations on point cloud surfaces,” *SIAM J. Sci. Comput.* **45**(2), A312-A337.
- [15] Kansa, E.J. [1990] “Multiquadrics—A scattered data approximation scheme with applications to computational fluid dynamics—II solutions to parabolic, hyperbolic and elliptic partial differential equations,” *Comput. Math. Appl.* **19**(8–9), 147-161.
- [16] Wright, G.B., Fornberg, B. [2006] “Scattered node compact finite difference-type formulas generated from radial basis functions,” *J. Comput. Phys.* **212**(1), 99–123.
- [17] Chandhini, G., Sanyasiraju, Y.V.S.S. [2007] “Local RBF-FD solutions for steady convection–diffusion problems,” *Internat. J. Numer. Methods Engrg.* **72**, 352–378.
- [18] Fornberg, B., Flyer, N. [2015] “Solving PDEs with radial basis functions,” *Acta Numer.* **24**, 215–258.
- [19] Gunderman, D., Flyer, N., Fornberg, B. [2022] “Transport schemes in spherical geometries using spline-based RBF-FD with polynomials,” *J. Comput. Phys.* **408**, 109256.
- [20] Shahane, S., Radhakrishnan, A., Vanka, S.P. [2021] “A high-order accurate meshless method for solution of incompressible fluid flow problems,” *J. Comput. Phys.* **445**, 110623.

- [21] Sanyasiraju, Y.V.S.S., Chandhini, G. [2009] “A note on two upwind strategies for RBF-based grid-free schemes to solve steady convection–diffusion equations,” *Internat. J. Numer. Methods Fluids* **61**, 1053–1062.
- [22] N.B. Barik, T.V.S. Sekhar, An Efficient Local RBF Meshless Scheme for Steady Convection–Diffusion Problems, *Int. J. Comput. Methods* 14 (2017) 6 1750064.
- [23] Barik, N.B., Sekhar, T.V.S. [2021] “Mesh-free multilevel iterative algorithm for Navier–Stokes equations,” *Numer. Heat Transf. B: Fundam.* **79**(3), 150-164.
- [24] Liszka, T., Orkisz, J. [1980] “The finite difference method at arbitrary irregular grids and its application in applied mechanics,” *Comput. & Structures* **11**, 83-95.
- [25] Micchelli, C.A. [1986] “Interpolation of scattered data: distance matrices and conditionally positive definite functions,” *Const. Approx.* **2**, 11–22.
- [26] Franke, R. [1982] “Scattered data interpolation: tests of some methods,” *Math. Comput.* **38**, 181–200.
- [27] Barik, N.B., Sekhar, T.V.S. [2021] “A modified multilevel meshfree algorithm for steady convection-diffusion problems,” *Int. J. Numer. Meth. Fluids.* **93**(7), 2121-2135.